

Accretion-erosion conversion in the subaqueous Yangtze Delta in response to fluvial sediment decline

Luan, Hua Long; Ding, Ping Xing; Yang, Shi Lun; Wang, Zheng Bing

DOI

[10.1016/j.geomorph.2021.107680](https://doi.org/10.1016/j.geomorph.2021.107680)

Publication date

2021

Document Version

Final published version

Published in

Geomorphology

Citation (APA)

Luan, H. L., Ding, P. X., Yang, S. L., & Wang, Z. B. (2021). Accretion-erosion conversion in the subaqueous Yangtze Delta in response to fluvial sediment decline. *Geomorphology*, 382, 1-10. Article 107680. <https://doi.org/10.1016/j.geomorph.2021.107680>

Important note

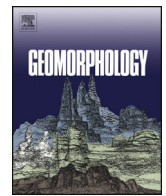
To cite this publication, please use the final published version (if applicable). Please check the document version above.

Copyright

Other than for strictly personal use, it is not permitted to download, forward or distribute the text or part of it, without the consent of the author(s) and/or copyright holder(s), unless the work is under an open content license such as Creative Commons.

Takedown policy

Please contact us and provide details if you believe this document breaches copyrights. We will remove access to the work immediately and investigate your claim.



Accretion-erosion conversion in the subaqueous Yangtze Delta in response to fluvial sediment decline

Hua Long Luan^{a,b,*}, Ping Xing Ding^{a,**}, Shi Lun Yang^a, Zheng Bing Wang^{a,c,d}

^a State Key Laboratory of Estuarine and Coastal Research, East China Normal University, Shanghai 200062, China

^b Changjiang River Scientific Research Institute, Wuhan 430010, China

^c Delft University of Technology, Faculty of Civil Engineering and Geosciences, 2628 CN Delft, the Netherlands

^d Deltares, 2600 MH Delft, the Netherlands

ARTICLE INFO

Article history:

Received 8 September 2019

Received in revised form 23 February 2021

Accepted 25 February 2021

Available online 2 March 2021

Keywords:

Accretion-erosion conversion

Fluvial sediment decline

Estuarine engineering projects

Yangtze Delta

ABSTRACT

Identifying the pattern of delta morphological change under decreasing sediment flux due to dam construction is essential for sustainable management in such densely populated coastal areas. In this study, we investigated the morphological processes of the Yangtze mouth bar and prodelta based on bathymetric data on a decadal-interannual scale (1958, 1978, 1997, 2002, 2007, 2010, 2013 and 2015). We found that strong accretion ($205.1 \text{ Mm}^3 \text{ yr}^{-1}$) occurred during 1958–1978, when a high sediment load (465 Mt yr^{-1}) was supplied by the Yangtze. Afterwards, the net accumulation rate decreased to $31.9 \text{ Mm}^3 \text{ yr}^{-1}$ in 1978–1997 and $114.6 \text{ Mm}^3 \text{ yr}^{-1}$ in 1997–2002 as a result of riverine sediment loads decreasing to 390 Mt yr^{-1} and 314 Mt yr^{-1} , respectively. Surprisingly, the net accumulation rate increased to $130.8 \text{ Mm}^3 \text{ yr}^{-1}$ in 2002–2007, though the sediment load sharply decreased to 177 Mt yr^{-1} . This anomaly was attributed to the construction of training walls within the mouth bar area, which induced significant accretion in groyne-sheltered areas and nearby regions. Along with a further decrease in sediment load, the entire study area converted to net erosion of $-200.4 \text{ Mm}^3 \text{ yr}^{-1}$ in 2007–2010 and $-152.2 \text{ Mm}^3 \text{ yr}^{-1}$ in 2010–2013. Stronger erosion in the former period was partly caused by intensive dredging activities in the mouth bar area. The critical sediment discharge for the Yangtze mouth bar and prodelta to retain net accretion was estimated to be ca. 218 Mt yr^{-1} . If deducting the impacts of estuarine engineering projects on accretion/erosion during 1997–2010, the critical sediment discharge is adjusted to ca. 234 Mt yr^{-1} . In combination with previously reported accretion-erosion conversion elsewhere in the Yangtze Delta, we inferred that most portion of the subaqueous delta has most likely converted from net accretion to net erosion in response to fluvial sediment decline, and the mouth bar area showed the latest conversion among portions of the delta. Integrated assessment and adaptive strategies are urgently required for the Yangtze Delta to survive the coming erosional stage.

© 2021 Elsevier B.V. All rights reserved.

1. Introduction

River deltas hold both social-economic and environmental significance due to the dense population and productive ecosystems within these dynamic systems (Syvitski and Saito, 2007). As the river-ocean interface, terrestrially derived sediments accumulate at river mouths, forming one of the most active deposition sites on Earth (Wright, 1977). Morphodynamics of river mouths are of high importance in terms of infrastructure safety, resource utilization, navigation maintenance and ecological service function. However, most of the world's

river mouths are at risk of or currently suffering from erosion and flooding due to insufficient sediment supply and relative sea-level rise (Syvitski et al., 2009). To cope with this risk, understanding morphological patterns of river mouths in response to fluvial sediment decline and the evolution trends has recently become an issue of global concern (Giosan et al., 2014; Tessler et al., 2015; Day et al., 2016).

Previous studies have widely identified river delta degradation under diminishing sediment supply in terms of shoreline recession (White and El Asmar, 1999; Chu et al., 2006; Anthony et al., 2015) and intertidal wetland loss (Morton et al., 2005; Yang et al., 2005), whereas knowledge on the morphological response of mouth bar areas and subaqueous deltas is limited. Because of different natural conditions and human interventions, river deltas may show diverse morphological patterns under fluvial sediment decline. For instance, sediment trapping in the Mississippi River basin has induced severe drowning of the delta plain and subaqueous delta retrogradation (Blum and Roberts, 2012;

* Correspondence to: H.L. Luan, Changjiang River Scientific Research Institute, Wuhan 430010, China.

** Corresponding author.

E-mail addresses: hluan@mail.crsri.cn (H.L. Luan), pxding@sklec.ecnu.edu.cn (P.X. Ding).

Maloney et al., 2018), while the Danube delta and São Francisco delta switched from seaward expansion to downdrift migration with substantial decline of depositional rates after sediment entrapment in upstream reservoirs (Bittencourt et al., 2007; Preteasa et al., 2016). Large river deltas in China also showed various patterns under human interventions. For instance, both the Yellow River delta and the Pearl River delta converted to net erosion at the subaqueous deltas due to insufficient sediment supply (Jiang et al., 2017; Wu et al., 2018), while land reclamation played an important role in subaqueous topographic changes in the Qiantang Estuary (Xie et al., 2017). Therefore, a number of case studies of river mouth bars and subaqueous deltas are required to better understand the processes of morphological evolution under fluvial sediment decline.

As one of the world's most important social-economic centers, the large-scale Yangtze Delta experienced a sharp reduction in river sediment discharge in recent decades, particularly after the closure of the Three

Gorges Dam (TGD) in 2003 (Yang et al., 2015). Thus, this area provides a typical example to address this issue (Fig. 1). Several studies have revealed accretion-erosion conversion of the mouth bar area and subaqueous delta due to fluvial sediment decline. For instance, Yang et al. (2011) and Du et al. (2016) demonstrated that a rectangular portion (~1800 km²) of the subaqueous delta had converted from accretion to erosion since 2000, and Luo et al. (2017) found delta recession within a domain of less than 1000 km² at the northernmost outlet of the delta. Because the Yangtze mouth bar area and subaqueous delta have an area of nearly 10,000 km² (Chen et al., 1985), the study areas considered above are too small to represent the overall pattern of the Yangtze Delta. Although Dai et al. (2014) defined a larger study area spanning from the mouth bar to the adjacent subaqueous delta, they used only the bathymetric dataset before 2009 and concluded that the Yangtze mouth bar retained high accumulation until 2009. The amount of sediment accumulation in 2002–2009 was much higher than the river sediment discharge (SD), whereas

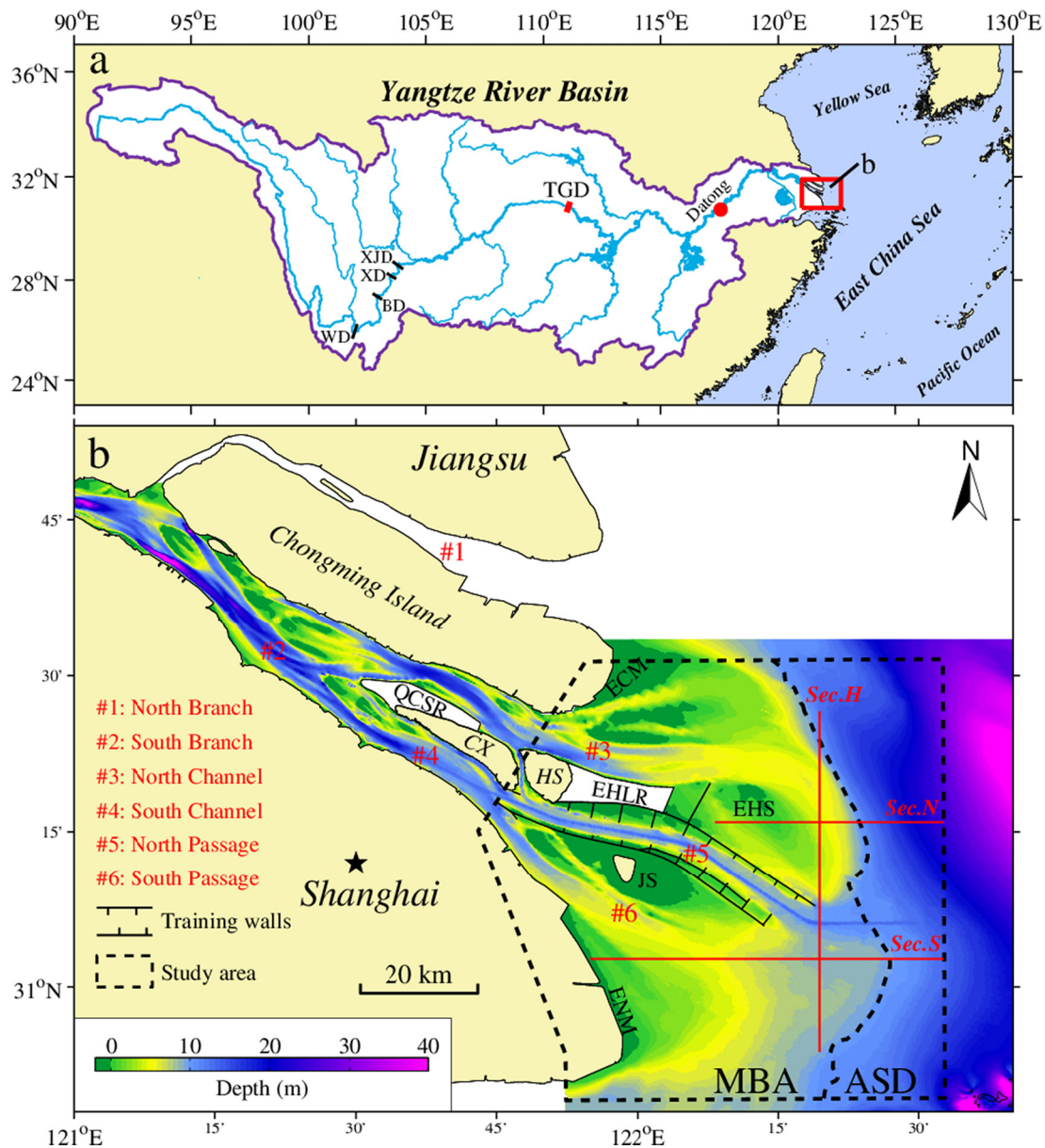


Fig. 1. (a) Map of the Yangtze River Basin and the location of the Yangtze Estuary (rectangle); (b) map of the Yangtze Estuary with bathymetry observed in 2010. The study area is divided into the mouth bar area (MBA) and adjacent subaqueous delta (ASD) by the 10 m isobath. TGD, XJD, XD, BD and WD represent the Three Gorges, Xiangjiaba, Xiluodu, Baihetan, and Wudongde dams, respectively; ECM: East Chongming Mudflat; EHS: East Hengsha Shoal; JS: Jiuduansha Shoal; ENM: East Nanhui Mudflat; CX: Changxing Island; HS: Hengsha Island; QCSR: Qingcaosha Reservoir; and EHLR: East Hengsha Land Reclamation.

the provenance of the excess sediment remained unknown. Therefore, it is imperative to further investigate the morphological response of a larger domain and use up-to-date data.

Our previous study on decadal morphological evolution of the Yangtze Estuary indicated that the mouth bar area was still characterized by net accretion in 1997–2010 (Luan et al., 2016). However, the morphological processes during this 13-year period were less revealed. Notably, the Deep Navigation Channel Project (DNCP), as one of the largest estuarine engineering projects in the world, was just implemented along the North Passage (NP) in this period (Fig. 1b). The superimposed impacts of fluvial sediment decline and large-scale estuarine engineering projects in the mouth bar area may complicate the morphological pattern at an interannual scale, which have been investigated in many recent studies using multiple approaches. Dai et al. (2013) used a multivariate technique to analyze bathymetric changes of the NP during 1998–2011 and found that the dredging-induced deepening of the thalweg and the construction of the T-shaped groin fields along the NP to improve and maintain the navigation channel was the predominant cause (85%) of bathymetric changes within the NP. By coupling GIS, geostatistics and remote sensing techniques, Li et al. (2016) demonstrated that the DNCP had substantial effects on the geometry of the adjacent Jiuduansha Shoal (JS). Wei et al. (2016) analyzed morphological evolution of the JS in 1998–2014, which showed that the DNCP induced continuous northward shoal expansion. Wei et al. (2017, 2019) also pointed out that the retreat in the north and progradation around the cusp of the East Nanhui Mudflat (ENM) resulted from the DNCP-induced increase in ebb flow intensity in the South Passage (SP). Besides, Zhu et al. (2016) set up a hydrodynamic model and indicated that the recent erosion of the southern subaqueous delta can be related to the DNCP. Previously, we conducted a process-based morphological modeling study and identified the physical mechanism between the DNCP and the accretion/erosion patterns at adjacent shoals and the subaqueous delta (Luan et al., 2017, 2018). A recent study by Zhu et al. (2019) examined the morphological changes of the East Hengsha Shoal (EHS) and JS in the mouth bar area and suggested that the morphodynamic response time of the mouth bar area to fluvial sediment decline was over 30 years (starting from the mid-1980s). They argued that the study area can retain net accretion under fluvial sediment decline since the observed accretion rate in 2013–2016 was at the same level with that in the 1980s, and attributed erosion in 2007–2013 to dredging activities and the construction of the training walls. This viewpoint was probably tenable for the shoals rather than the entire mouth bar area. Furthermore, the dredging amount in 2002–2013 only accounted to limited proportion of observed erosion volumes as showed by Zhu et al. (2019). These previous studies indicated that human interventions resulted in highly variable morphological patterns within different parts of the mouth bar area (Supplementary Fig. S1, online), whereas the accretion/erosion status of the major mouth bar system and different sensitivities within the entire subaqueous delta to fluvial sediment decline were poorly investigated. Moreover, rare studies have quantitatively separated the interference of estuarine engineering projects from observed morphological pattern, particularly in terms of the morphological tipping point of the mouth bar system.

This study analyzes the bathymetric data at a decadal-interannual scale (1958, 1978, 1997, 2002, 2007, 2010, 2013 and 2015) covering the major Yangtze mouth bar and prodelta with a total area of over 4900 km². Our major objective is to determine whether the delta has converted from net accretion to net erosion on a large spatial scale, and to quantify the relationship between the net accumulation rate and SD with/without the impacts of estuarine engineering projects. The critical SD for the accretion-erosion conversion is estimated and discussed. Understanding the patterns of morphological evolution of the Yangtze Delta provides not only scientific support for the sustainable management of this large-scale dynamic system, but can also shed light on the evolutionary mechanisms of other tidal-influenced river deltas under changing fluvial sediment supplies.

2. Yangtze Delta and its mouth bar area

The Yangtze River, which is the third largest river in the world (Milliman and Farnsworth, 2011), reaches its mouth near Shanghai City and enters the inner shelf of the East China Sea. The Yangtze Delta is an actively depositional and progradational system that has had an abundant fluvial fine sediment supply over the past 5000 years (Hori et al., 2001), resulting in the present large-scale deltaic system (Fig. 1a). Currently, the Yangtze Delta is approximately 90 km wide spanning from the North Branch to the SP and extends seaward for nearly 100 km to the ancient valley (~50 m) with a slope of the delta front of 0.6%–1.0% (Hori et al., 2001). The mouth bar area, which is characterized by straight and wide channels adjacent to extensive intertidal flats, connects to the subaqueous delta from the channel outlets (Fig. 1b). The mean depth of the mouth bar crests is approximately 6 m, which is shallower than those of both the upstream and downstream channels (Chen et al., 1999). The seabed in the mouth bar area is dominated by cohesive mud, which is frequently resuspended by tidal currents (Liu et al., 2010; Luo et al., 2012). This area behaves as both the estuarine turbidity maxima and the depocenter of the river mouth (Chen et al., 1985; Dai et al., 2014).

Prior to the 1970s, huge amounts of fresh water (900 km³ yr⁻¹) and fluvial sediment (470 Mt yr⁻¹) reached the Yangtze Delta, ranking 4th and 5th around the world in these two categories, respectively (Milliman and Farnsworth, 2011). No significant variation trend has been observed for the annual water runoff in the past half-century, while the annual sediment load has gradually decreased since the 1970s (Fig. 2). The mean SD during the first decade after the closure of the TGD in 2003 dropped to a relatively low level (145 Mt yr⁻¹), which was only approximately 30% of the value in 1950–1968 (Yang et al., 2015). The river water and sediment discharge showed strong seasonal variations, with approximately 71% of the annual runoff and 87% of the annual sediment load delivered to the mouth during the flood season from May to October (Chen et al., 2007). The astronomical tide around the Yangtze mouth bar area is irregular and semidiurnal, with mean and maximum tidal ranges of 2.66 and 4.62 m, respectively (Yun, 2004). The mean height of wind-induced waves around the mouth bar area is 0.9 m under normal weather conditions. Fluvial sediment mainly includes fine suspensions, with a median grain size of ~10 μm (Yang et al., 2018a).

Morphodynamics of the Yangtze Delta are primarily controlled by combined river and tidal forcing (Guo, 2014), while wind waves only seasonally shape the morphology of shallow shoals at the delta front (Zhang et al., 2018). Although the Yangtze Delta has maintained its three-level bifurcation and four-outlet configuration under fluvial sediment decline since the 1950s, remarkable erosion and accretion occurred in the bifurcation channels and intertidal flats (Yun, 2004; Yang et al., 2005; Luan et al., 2016). Human interventions, including altering river water and sediment discharge in the catchment and constructing engineering projects in the estuary, have played an

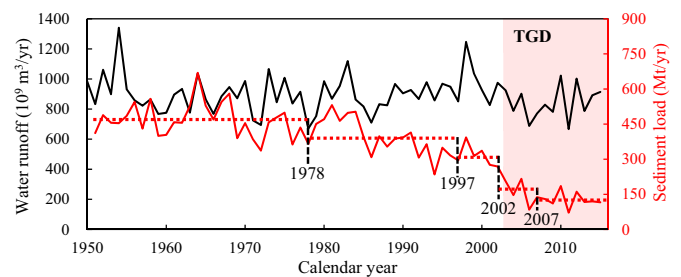


Fig. 2. Variations in annual river runoff (black line) and sediment load (red line) at Datong station (tidal limit) since 1950. The shaded area denotes the period since the closure of the Three Gorges Dam (TGD) in 2003.

increasingly important role in recent decades (De Vriend et al., 2011; Wang et al., 2015). One of the largest estuarine engineering projects is the DNCP, which was constructed along the NP to improve the navigation capacity (Fig. 1b). The DNCP was implemented from 1998 to 2010 including three phases and involved the construction of twin dikes and 19 perpendicular groynes with a total length of 100.7 km. The upstream half of the training walls were constructed along the NP in Phase I (1998–2001) and then extended to the present configuration in Phase II (2002–2005). Intensive dredging was carried out to deepen the navigation channel from 6.5 m in 1997 to 8.5 m in 2001, to 10 m in 2005 and finally to 12.5 m in 2011. Thus, the mouth bar in the NP was cut through artificially. Other engineering projects within the mouth bar area include land reclamation at the EHS and the ENM (Supplementary Fig. S2, online).

3. Methods

Bathymetric data observed in various years (1958, 1978, 1997, 2002, 2007, 2010, 2013 and 2015) were collected (Supplementary Table S1, online). Though the measuring time was 1976–1978 for the bathymetry map 1978, most of the study domain was recorded in 1978 and the periods 1958–1978 and 1978–1997 were much longer than the following periods. The soundings of each year, referenced to the theoretical lowest-tide datum at Wusong, were interpolated into a grid through the Surfer mapping software package. Subsequently, a digital elevation model (DEM) was generated for each year of bathymetric data (Supplementary Fig. S3, online). The erosion/deposition patterns were obtained by subtracting a later DEM from an earlier one. Since the North Branch received less than 5% of river discharge and sediment load in the study period, and bathymetric data at the mouth of the North Branch before the 1990s was unavailable, the North Branch was excluded in the present study. A polygonal domain was defined as the study area for erosion/deposition calculations (Fig. 1b). The concerned domain covers the mouth bar area and prodelta, which were bounded by the 10 m isobath in 1997 and analyzed separately. Changes in sediment volume and thickness were calculated based on the differences between DEMs. Three typical sections were extracted from the DEM to describe the amplitudes of bed-level changes at subaqueous slopes.

The calculation error is primarily determined by the measurement accuracy and density, grid size and interpolation method (Duan, 2012). The bathymetry measurements were implemented by echo sounder with a vertical error of approximately 0.1 m. The sounding positions were recorded by a theodolite for the 1958 and 1978 charts and a GPS (Trimble Navigation Limited, California, USA) for the remaining years, and the corresponding errors were 50 m and <1 m, respectively. Generally, these errors are acceptable for calculating erosion and accretion volume because of significant bed-level changes over decadal time scales (Luan et al., 2016). The bathymetry map scales range from 1:10,000 to 1:130,000 (Supplementary Table S1, online) and are mostly higher than 1:50,000. The density of depth samples is sufficient for the calculation of morphological changes (Dai et al., 2014; Luo et al., 2017). The Kriging interpolation was applied in Surfer. Many previous studies have verified that this method was optimal among all other methods and this method has been widely used for calculating morphological evolution of deltas and estuarine regions (Van der Wal et al., 2002; Blott et al., 2006; Jaffe et al., 2007). The grid size should be smaller than the distance of adjacent depth points, and a 50 × 50 m grid was chosen after a series of interpolation tests. Because of land reclamation at the EHS and ENM, areas with available bathymetric data vary from 4904 km² in 1958 to 4574 km² in 2013 (Supplementary Fig. S3, Table S2, online). The total area for the period of 2007–2013 was the smallest which was only ~6.7% lower than the largest area in 1958–1997. Most of decreased area were intertidal flats (EHS and JS), and bed-level changes at these flats were usually slow. Therefore, it is suggested that the impact of the area difference on the analysis of sediment volume changes and morphological patterns is negligible. Due to the

data availability, the area of the bathymetry data in 2015 was only 62% of that in 2013, and sediment volume change in 2013–2015 was not compared with others.

4. Results

4.1. Erosion/deposition patterns during 1958–2015

The study area includes three outlets, viz. North Channel, NP and SP, and adjacent intertidal mudflats, viz. East Chongming Mudflat (ECM), EHS, JS and ENM (Fig. 1b). The morphology characterized by channels and intertidal shoals/mudflats in the Yangtze mouth bar area has been maintained since 1958, although local changes were remarkable (Supplementary Fig. S3, Table S2, online). Land reclamation at the ECM, EHS and ENM significantly decreased the intertidal areas within the mouth bar area. A deep navigation channel along the NP was formed after 2002 due to the construction of training walls and intensive dredging activities.

The erosion/deposition patterns during 1958–2013 indicate that the Yangtze mouth bar and delta-front system show apparent accretion-erosion conversion (Fig. 3). Under high river sediment discharge in 1958–1978, strong deposition occurred in the shallow shoals and the subaqueous delta, while erosion was only found in limited areas (Fig. 3a). The pattern in 1978–1997 featured distinct spatial variations (Fig. 3b). The intertidal shoals (ECM, EHS and JS) and the subaqueous delta near the EHS continued to accrete, whereas the main channels and the northern subaqueous delta experienced erosion. The evolution pattern in 1997–2013 was produced to retain the decadal timescale as the first two periods. The pattern showed that significant accretion occurred in the groyne-sheltered areas and on the intertidal flats, while erosion was found at the subaqueous delta along the delta front (Fig. 3c). The main contributor for these evolution features is the construction of training walls overlapping fluvial sediment decline (Luan et al., 2018).

Considering the construction phases of the DNCP, the decadal period 1997–2015 was divided into five short periods to capture the engineering-induced interferences on the medium-term bed-level changes. In 1997–2002, the upper part of both the NP and SP showed erosion as the first phase of the DNCP was completed in 2001 (Fig. 3d). Meanwhile, the northern subaqueous delta rebounded to accretion, and the southern area was under a state of transition with slight erosion (Fig. 3d). As the training walls were extended to the present location in 2005 in the second phase, severe deposition occurred in groyne-sheltered areas along both sides of the NP in 2002–2007 (Fig. 3e). Accretion at the EHS peaked in 2002–2007 and decreased afterwards. Intensive dredging activities in the third phase induced remarkable deepening along the navigation channel as shown in the evolution pattern during 2007–2010 (Fig. 3f). The area experiencing erosion showed a gradual increase after 1997. The mouth bar area and prodelta have been dominated by overall erosion since 2007 (Fig. 3f–h).

Three typical sections, as shown in Fig. 1b, represent the subaqueous slopes at the EHS (Sec. N), the ENM and SP (Sec. S) and the delta front (Sec. H). Variations of Sec. N and Sec. H indicate that the EHS grew higher during 1997–2013 (Fig. 4a, c), and the depths at its center area and southeast end decreased by approximately 2 m and 3.5 m, respectively (Fig. 4d). The variation of Sec. S indicates that the high intertidal flat at the ENM (<2 m) accreted continuously, while its lower part (2–6 m) converted from accretion to erosion after 2010 (Fig. 4b). The variation of Sec. H indicates that the navigation channel at the mouth of the NP was deepened by more than 5 m from 1997 to 2013 (Fig. 4c, d). The subaqueous delta at the mouths of both the North Channel and SP underwent erosion, and the water depths increased by nearly 2 m in the northern area and 2.5 m in the southern area (Fig. 4d).

4.2. Sediment accumulation rates

Sediment accumulation rates within the study area can provide a quantitative assessment of morphological changes. The calculation

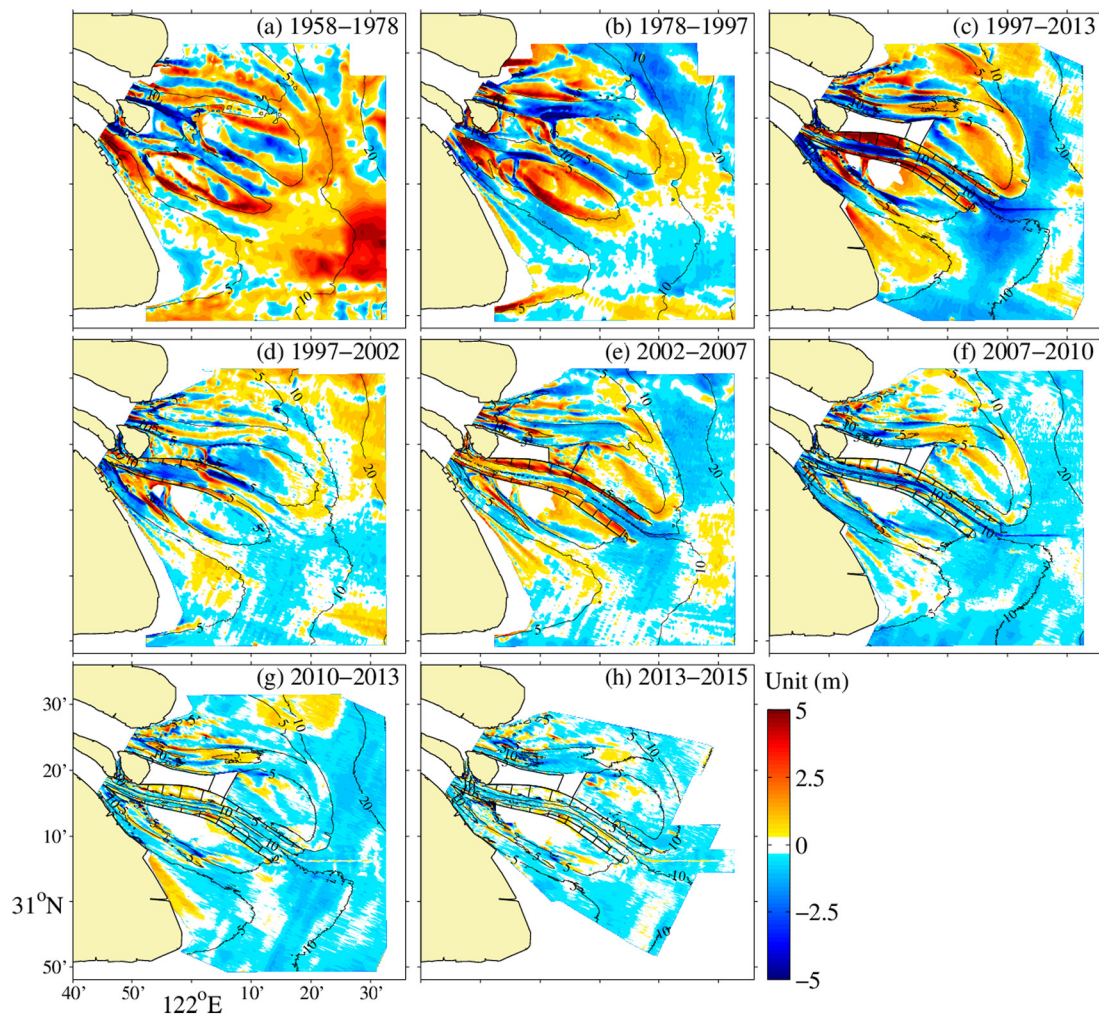


Fig. 3. Erosion/deposition patterns of the Yangtze mouth bar area and subaqueous delta in different periods during 1958–2015. The isobaths in the latter year are presented in each panel.

result of the Yangtze mouth bar and prodelta as defined in Fig. 1b was $205.1 \text{ Mm}^3 \text{ yr}^{-1}$ in 1958–1978, which was the highest during the study period (Fig. 5a; Supplementary Table S2, online). In the following periods, the accumulation rate decreased sharply to $31.9 \text{ Mm}^3 \text{ yr}^{-1}$ in 1978–1997 and $16.8 \text{ Mm}^3 \text{ yr}^{-1}$ in 1997–2013. During the four short periods after 1997, the accumulation rate increased to $114.6 \text{ Mm}^3 \text{ yr}^{-1}$ in 1997–2002 and $130.8 \text{ Mm}^3 \text{ yr}^{-1}$ in 2002–2007. Afterwards, the entire study area converted to strong erosion with the sediment accumulation rate of $-200.4 \text{ Mm}^3 \text{ yr}^{-1}$ in 2007–2010 and $-152.2 \text{ Mm}^3 \text{ yr}^{-1}$ in 2010–2013 as the SD decreased to a low level (141 Mt yr^{-1} in 2007–2010 and 134 Mt yr^{-1} in 2010–2013). In 2013–2015, the SD further decreased to 118 Mt yr^{-1} , and 62% of the entire study area still showed net erosion ($-64.4 \text{ Mm}^3 \text{ yr}^{-1}$). Thus, though the entire study area was under a status of net sediment accumulation at a decadal interval (1997–2013), the accretion-erosion conversion has already occurred since 2007. Notably, relative sea-level rise since the 1950s at the Yangtze Delta ranged from 4.8 mm/a to 6.5 mm/a after synthesizing published China Sea Level Bulletin and previous studies on land subsidence and sea-level rise (Wu et al., 2003; Wang et al., 2012). This range only accounted to 3.6%–9.6% of mean erosion thickness and 3.9%–9.1% of mean deposition thickness (Supplementary Table S2). It is suggested that relative sea-level rise cannot produce substantial effect on the accuracy of results.

Considering the strong spatial variation of the morphological changes, the study area was divided into the mouth bar area and adjacent subaqueous delta by the 10 m isobath (Fig. 1b). The mouth bar area experienced gradual decrease in net accretion rate at a decadal

timescale during 1958–2013 (Fig. 5b), which was consistent with the variation trend of the entire study area. The accumulation rate in 1958–1978 was $125.5 \text{ Mm}^3 \text{ yr}^{-1}$, accounting for over 61% of the net accretion volume of the entire study area. Afterwards, the accumulation rate dropped to $46.0 \text{ Mm}^3 \text{ yr}^{-1}$ in 1978–1997 and $21.7 \text{ Mm}^3 \text{ yr}^{-1}$ in 1997–2013. In shorter time spans after 1997, the mouth bar area was nearly at an equilibrium status ($0.5 \text{ Mm}^3 \text{ yr}^{-1}$) in 1997–2002, and then rebounded to strong accretion ($171.0 \text{ Mm}^3 \text{ yr}^{-1}$) in 2002–2007. Over 95% of accretion occurred in the groyne-sheltered areas within the NP ($94.1 \text{ Mm}^3 \text{ yr}^{-1}$) and at the EHS ($68.7 \text{ Mm}^3 \text{ yr}^{-1}$) due to the construction of training walls (Fig. 3e). Overall erosion occurred in the mouth bar area after 2007 with the net accumulation rate of $-139.9 \text{ Mm}^3 \text{ yr}^{-1}$ in 2007–2010 and $-64.0 \text{ Mm}^3 \text{ yr}^{-1}$ in 2010–2013. Intensive dredging activities induced $-43.0 \text{ Mm}^3 \text{ yr}^{-1}$ of erosion in 2007–2010 along the navigation channel, and the latter partly explained the higher net erosion rate in 2007–2010 than that in the latter period.

Adjacent subaqueous delta also showed strong accretion in 1958–1978 ($79.6 \text{ Mm}^3 \text{ yr}^{-1}$), and converted to slight erosion in 1978–1997 and 1997–2013 (Fig. 5b). Notably, remarkable net accretion occurred in 1997–2002. Afterwards, the adjacent subaqueous delta experienced increasing erosion under low fluvial sediment supply. The net erosion rate was $40.3 \text{ Mm}^3 \text{ yr}^{-1}$ in 2002–2007 and increased to $60.5 \text{ Mm}^3 \text{ yr}^{-1}$ in 2007–2010 and $88.2 \text{ Mm}^3 \text{ yr}^{-1}$ in 2010–2013. Besides, the net erosion thickness of the adjacent subaqueous delta was larger than the value of the mouth bar area in 2007–2010 and 2010–2013 (Supplementary Table S2, online), suggesting stronger erosion intensity of the

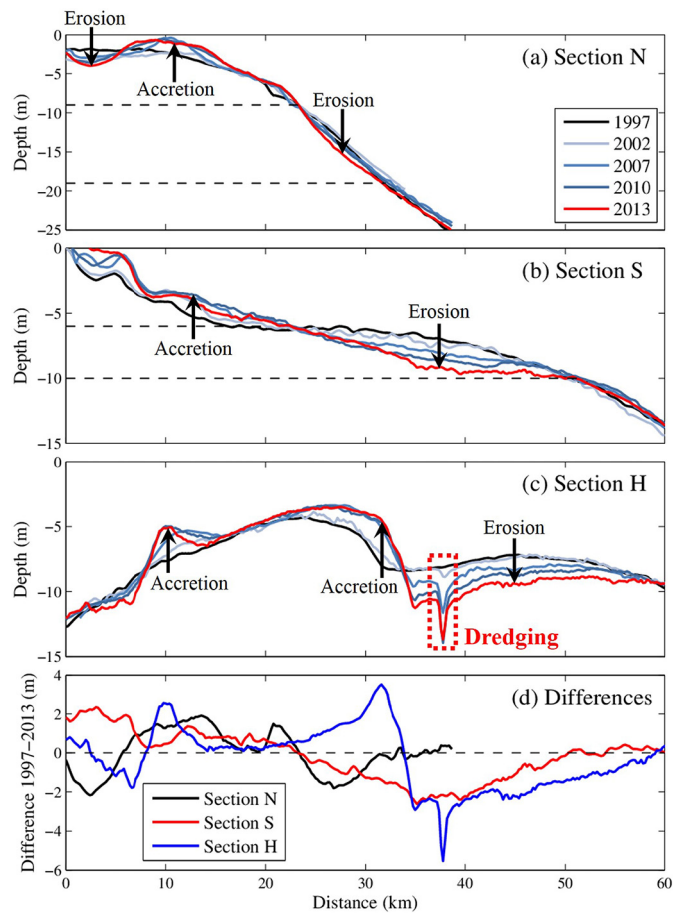


Fig. 4. (a–c) Variations in three typical sections from 1997 to 2013; (d) differences in the sections between 1997 and 2013. The locations of the sections are shown in Fig. 1b. Sec. N and Sec. S are heading seaward and Sec. H is heading southward. The depth refers to the theoretical lowest tidal datum. Positive values represent accretion, and negative values represent erosion in (d).

subaqueous delta than the mouth bar area. The above results also indicate that the adjacent subaqueous delta converted from net accretion to erosion around 2002, which was earlier than the conversion of the mouth bar area (Fig. 5b).

5. Discussion

5.1. Primary cause of the accretion-erosion conversion in the Yangtze mouth bar area

Our results support previous studies in that the accumulation rate in the Yangtze subaqueous delta decreased during 1977–1997 (Yang et al., 2003) and the accretion-erosion conversion occurred after the closure of the TGD in 2003 (Yang et al., 2011; Du et al., 2016). Moreover, we find that the major mouth bar and prodelta (nearly 5000 km² in area) converted from net accretion to net erosion since 2007. Several abnormal changes in sediment accumulation rates were identified in the accretion-erosion conversion process. For instance, the accumulation rate in 1978–1997 was lower than that of the following period (1997–2002). This was probably attributable to the typhoon event in 1997 (Dai et al., 2014), since the bathymetric data of 1997 was observed by the end of the year and recorded the morphological impacts of the No. 9711 typhoon, which passed through the Yangtze Delta in Aug. 1997. The adjacent subaqueous delta rebounded to intensive net accretion in 1997–2002, and this was probably because of the rapid recovery from typhoon-induced erosion. Although the study area showed net

sediment accumulation during 1997–2013, the accretion mainly occurred in 2002–2007 immediately after the construction of training walls. As the morphological impacts of training walls on the local and adjacent areas gradually diminished after 2007, erosion became dominant (Fig. 3f, g) under low fluvial sediment supply (<150 Mt yr⁻¹). The overall erosion in the entire study area was unlikely to reflect a short-term adjustment process.

Generally, progradation or regression of river deltas depends on the sediment budget between the riverine supply and offshore dispersal (Syvitski and Saito, 2007; Canestrelli et al., 2010). Previous studies based on seismic profiles and sediment cores have demonstrated that the Yangtze mouth bar and delta-front system was a sediment accumulation area in the Holocene (Stanley and Chen, 1993; Liu et al., 2007). A recent observation-based study by Deng et al. (2017) suggested that the coastal currents passing through the Yangtze Delta are estimated to deliver approximately 270 Mt yr⁻¹ of sediment southward, which was much higher than the present SD. Tidal currents at the delta front produced higher bed shear stress during peak tidal phases than the critical shear stress required for surficial sediment erosion, resulting in an erodible seabed (Yang et al., 2017). The deposition flux decreased with decreasing suspended sediment concentration due to fluvial sediment decline, and the deposition flux was lower than the erosion flux that initiated delta erosion. A recent study by Yang et al. (2020) also demonstrated delta-front erosion in 2003–2013 in terms of cross-shore elevation profiles and sediment budget in the Yangtze Delta, and they found that eroded sediment from the delta front compensated the effects of fluvial sediment decline on salt marshes. Therefore, it can be concluded that the primary cause of accretion-erosion conversion is that fluvial sediment supplied to the mouth bar area decreased to below the amount of sediment carried away by coastal currents. Erosion of the major Yangtze mouth bar and prodelta seems to be an inevitable tendency.

5.2. Interference of estuarine engineering projects

Large-scale estuarine engineering projects within the mouth bar area, i.e. the DNCP, affected morphological changes in both local and adjacent areas (Luan et al., 2016). Accretion within the groyne-sheltered areas along both sides of the NP was clearly due to the construction of the training walls, which induced a significant decrease in flow velocity and subsequent sediment settling during 2002–2007 (Fig. 3e). Afterwards, accretion within all groyne-sheltered areas was significantly decreased or even vanished in some areas, as shown in the erosion/deposition patterns in 2007–2010 and 2010–2013 (Fig. 3f, g). Therefore, the accretion amount within the groyne-sheltered areas in 2002–2007 (94.1 Mm³ yr⁻¹) is considered as the DNCP-induced (Fig. 5b). Meanwhile, intensive dredging activities induced -9.9 Mm³ yr⁻¹ of erosion in 2002–2007 and -43.0 Mm³ yr⁻¹ of erosion in 2007–2010 along the navigation channel (Fig. 5b).

The adjacent intertidal shoals and the subaqueous delta were also heavily impacted by the DNCP. The nearest intertidal shoals to the training walls are the EHS and JS in the northern and southern sides, respectively. Before 2002, most seaward parts of both the EHS and JS involved erosion (Fig. 3d). During 2002–2007, the training walls were extended to the present configuration and remarkable accretion occurred at the EHS and JS (Fig. 3e). After 2007, both shoals converted back to erosion-dominant (Fig. 3f). Continuous northward expanding of the JS was also induced by the DNCP (Wei et al., 2016), which has already been included in the groyne-sheltered areas. The retreat in the north and progradation around the cusp of the ENM resulted from the DNCP-induced increase in ebb flow intensity (Wei et al., 2017, 2019). Previous studies by Zhu et al. (2016) revealed that the presence of the training walls accelerated erosion at the southern subaqueous delta. Therefore, morphological impacts of the DNCP on adjacent areas in 2002–2007 included the EHS, JS, ENM and adjacent subaqueous delta. Quantification the DNCP-induced accretion/erosion refers to the

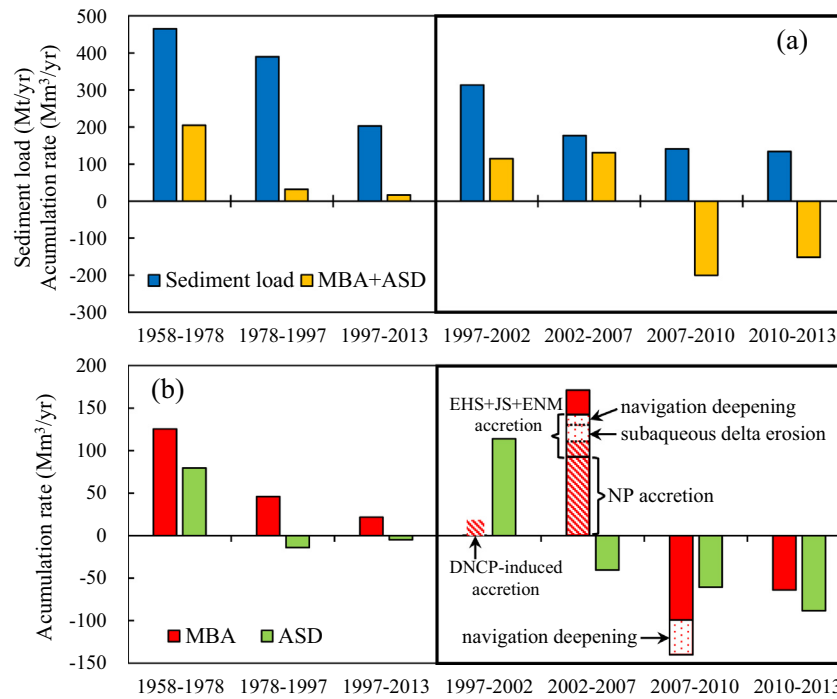


Fig. 5. (a) Annual-mean sediment load at Datong station and net accumulation rates of the entire study area as shown in Fig. 1b; (b) net accumulation rates of the mouth bar area (MBA) and adjacent subaqueous delta (ASD) as shown in Fig. 1b.

difference of bathymetry changes with and without training walls. Based on the above analysis of observed morphological changes, the process-based numerical model (Delft3D) was applied to simulate morphological changes of the Yangtze Estuary, and details of the model setup have been described in our recent research (Luan et al., 2018). According to the model results for the Phase II of the DNCP (2002–2007), the DNCP-induced accretion volumes at the EHS, JS and ENM were calculated as 25.7 Mm³ yr⁻¹, 13.6 Mm³ yr⁻¹ and 12.2 Mm³ yr⁻¹, respectively, and the DNCP-induced erosion volume at southern adjacent subaqueous delta was calculated as -20.7 Mm³ yr⁻¹ (Fig. 5b). The morphological impact of the training walls constructed during the Phase I (1997–2002) was simulated additionally. Model results showed that the training walls mainly enhanced accretion in the entrance of the NP and erosion in the entrance of the SP. The net volume difference was calculated as 19.9 Mm³ yr⁻¹ (Fig. 5b).

One important issue for delta protection and restoration is to characterize the morphological tipping points to avoid unfavorable changes in advance (Renaud et al., 2013). Here, we estimate the critical SD of the Yangtze mouth bar and prodelta to retain net accretion based on the relationship between the net accumulation rate and the SD at Datong station (the tidal limit). Considering the data in all study periods, a logarithmic fitting line was produced (correlation coefficient $R^2 = 0.58$), and the critical SD corresponding to neither accretion nor erosion was ca. 218 Mt yr⁻¹ (Fig. 6). If deducting the DNCP-induced accretion/erosion (including dredging) in 1997–2010 as calculated above, the net accumulation rates of the entire study area in 1997–2002, 2002–2007 and 2007–2010 would be changed to 94.7 Mm³ yr⁻¹, 15.7 Mm³ yr⁻¹ and -157.4 Mm³ yr⁻¹, respectively. Another logarithmic fitting line with an R^2 of 0.81 was derived using the modified data (Fig. 6), and the critical SD was adjusted to ca. 234 Mt yr⁻¹. It is suggested that estuarine engineering projects increased the resistance of the Yangtze mouth bar and prodelta against erosion under fluvial sediment decline. Therefore, the interference of estuarine engineering projects on delta response to fluvial sediment decline was quantified in terms of the occurrence time and the critical SD of accretion-erosion conversion.

A series of land reclamation projects had been carried out at the ENM and EHS since 1997 (Supplementary Fig. S2b, online). The accumulated sediment in reclaimed intertidal areas was not considered due to a lack of bathymetric data in these areas (Supplementary Fig. S3, online). Liu and Cui (2019) calculated the total siltation volume at the ENM, i.e., 60 Mm³ in 2002–2007 and 34.9 Mm³ in 2007–2013, and approximately 150 Mm³ of dredged sediment was used through pipelines for the siltation promotion project in the EHS in 2007–2010. Besides, a basic assumption of the above estimation is that fluvial sediment behaves as the major source for accretion of the Yangtze mouth area and prodelta. However, based on a hydrodynamic modeling study, Zhu

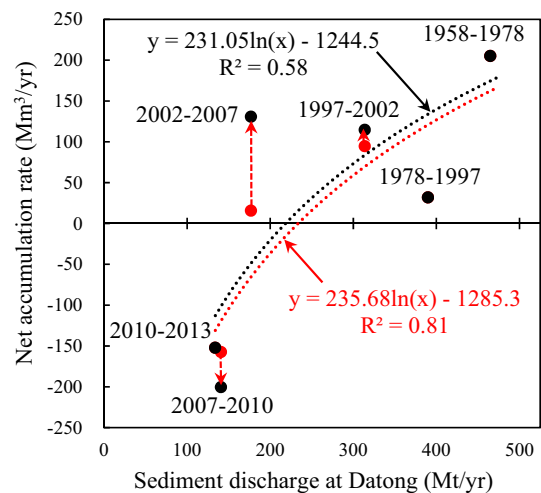


Fig. 6. Relationship between net accumulation rate of the entire study area (defined in Fig. 1b) and sediment discharge at Datong. Red dots represent the net accumulation rates without the impacts of estuarine engineering projects in 1997–2002, 2002–2007 and 2007–2010. The black and red dash fitting lines are derived by data with and without the impacts of estuarine engineering projects, respectively.

et al. (2016) indicated that the sediment required for the accretion in the mouth bar area may partly originate from the offshore muddy area. Luan et al. (2018) applied a process-based morphodynamic model and further confirmed that the presence of training walls enhanced the sediment transport from the subaqueous delta to the NP. It is suggested that the estimated critical SD could be even lower when taking land reclamation and offshore sediment supply into account.

5.3. Overall accretion-erosion conversion in the subaqueous Yangtze Delta

Previous studies reported accretion-erosion conversion in other areas of the subaqueous Yangtze delta. Specifically, accretion-erosion has occurred in the inner Yangtze Estuary including the South Branch, the South Channel and the upper North Channel (Luan et al., 2016), in the delta front out of the North Channel, North Passage and South Passage (Yang et al., 2011), in the North Branch and adjacent continental shelf (Dai et al., 2016; Luo et al., 2017; Yang et al., 2020), in the outer margin of the subaqueous Yangtze Delta (Luo et al., 2012), and in the southern area off the South Passage and the northern Hangzhou Bay (Yang et al., 2018b). Together with our findings from the mouth bar areas of the North Channel, North Passage and South Passage (Fig. 5), we conclude that overall accretion-erosion conversion has occurred in the subaqueous delta in response to fluvial sediment decline. Our conclusion is supported by observations that in recent years the amount of sediment transport away from the subaqueous Yangtze Delta by longshore currents (ca. 270 Mt yr⁻¹) was much greater than the sediment discharge from the Yangtze River (<150 Mt yr⁻¹) (Deng et al., 2017; Jia et al., 2018).

5.4. Causes of later accretion-erosion conversion in the mouth bar area than in other portions of the delta

Accretion-erosion conversion firstly occurred in the inner estuary in the 1980s (Luan et al., 2016), followed by the outer subaqueous delta off the North Branch since 1997 (Luo et al., 2017) and the delta front out of the North Channel, North Passage and South Passage around the year 2000 (Yang et al., 2011). This study has demonstrated that the mouth bar area converted from net accretion to net erosion after 2007. It is suggested that the sensitivity of the Yangtze Delta to fluvial sediment decline varies from the upstream to the outer delta. The lowest sensitivity of the mouth bar area to fluvial sediment decline among the entire delta is primarily determined by its intrinsic characteristics as a sediment accumulating site. Generally, a mouth bar area is located in the transition zone from fluvial-dominance to marine-dominance and from predominantly confined channels to receiving open waters. The expansion of flow and decrease in jet momentum flux lead to the deposition of sediment-laden channelized flow and consequently the formation of mouth bars (Wright and Coleman, 1974; Edmonds and Slingerland, 2007). Sediment trapping due to gravitational circulation, sediment resuspension, stratification-induced turbulence suppression and associated processes occur at the mouth area, forming the estuarine turbidity maxima (Jay and Musiak, 1994; Liu et al., 2010). The morphological pattern of the Yangtze Delta under decreasing sediment supply is representative of other marine-influenced river deltas. If the river-tidal dynamics and sediment properties of a deltaic system is similar to those of the Yangtze Delta, accretion-erosion conversion is most likely to occur in the inner tidal channel, the outer subaqueous delta and the mouth bar area in sequence.

5.5. Implication for future evolution trends and delta management

The morphological evolution of the Yangtze Delta has been influenced by both fluvial sediment decline and estuarine engineering projects, particularly since 1997. On the one hand, the Yangtze Delta showed a rapid morphological response to estuarine engineering projects (Dai et al., 2013; Luan et al., 2016; Wei et al., 2017). Most of the

groyne-sheltered areas have accreted at bed-levels above the theoretical lowest-tide datum, and the highest bed-level even exceeds the mean sea level. The remaining space for sediment deposition is becoming limited, suggesting that the morphological response to training walls is approaching equilibrium. With new land reclamation projects being implemented at the EHS and ENM in the future, sediment from the mouth bar area and subaqueous delta is likely to be continuously used for the creation of new land through further erosion. On the other hand, the decreasing SD has successively induced the erosion of the inner estuary (Luan et al., 2016), the subaqueous delta (Yang et al., 2011) and the mouth bar area (this study). Considering the integrated effects of the TGD, the Cascade Reservoirs in the upper Yangtze River Basin (Fig. 1a), the South-to North Water Diversion project and the riverbed erosion of the lower Yangtze River, the SD may further decrease to ~110 Mt yr⁻¹ in future decades (Yang et al., 2014). Yang et al. (2017) found that the uppermost 10–20 m of deposits in the subaqueous delta are relatively homogenous with nearly constant critical bed shear stress for erosion, and that these deposits can be erodible under peak tidal flows. The present study indicates that the largest erosion thickness of the mouth bar area and subaqueous delta is only ~2 m. Therefore, erosion of the Yangtze Delta, especially the subaqueous muddy area, is likely to continue in the coming decades until a dynamic equilibrium is reached. The erosion limit and timescale for approaching equilibrium are determined by the balance between the decreasing erosional ability of tidal currents due to continuous deepening and the increasing anti-erosional ability of the seabed due to armoring and sediment consolidation. Protection and sustainable management of the Yangtze Delta call for close attention to the threat posed by delta erosion to the safety of engineering facilities and ecosystems, as well as adaptive strategies.

6. Conclusions

The major Yangtze mouth bar and prodelta have converted from net accretion to net erosion since 2007 in response to fluvial sediment decline. Strong accretion (205.1 Mm³ yr⁻¹) occurred in 1958–1978 under a high sediment load (465 Mt yr⁻¹). Along with the decrease in SD after 1978, the accumulation rate decreased to 31.9 Mm³ yr⁻¹ in 1978–1997 and then increased to 114.6 Mm³ yr⁻¹ in 1997–2002 and 130.8 Mm³ yr⁻¹ in 2002–2007. Under a low sediment supply (<150 Mt yr⁻¹), net erosion was initiated after 2007 with an accumulation rate of –200.4 Mm³ yr⁻¹ in 2007–2010 and –200.4 Mm³ yr⁻¹ in 2010–2013. The mouth bar area showed a gradual decrease in the accumulation rate during 1958–2002. Only 0.5 Mm³ yr⁻¹ of sediment was accumulated in 1997–2002, implying that the mouth bar area was close to the tipping point. However, the mouth bar area rebounded to strong accretion (171.0 Mm³ yr⁻¹) in 2002–2007, which was also the main contributor to high accretion in the entire study area. Over 95% of the accretion occurred within the groyne-sheltered areas and at the EHS due to the construction of the training walls along the NP. The mouth bar area converted to net erosion after 2007, and the net accumulation rates were –139.9 Mm³ yr⁻¹ in 2007–2010 and –64.0 Mm³ yr⁻¹ in 2010–2013. Stronger erosion in the former period can be partly explained by intensive dredging (–43.0 Mm³ yr⁻¹) along the navigation channel. Based on the relationship between the net accumulation rates and the SD at Datong station, a critical SD to retain net accretion in the Yangtze mouth bar and prodelta was estimated to be ca. 218 Mt yr⁻¹. Deducing the morphological impacts of estuarine engineering projects, the critical SD was adjusted to ca. 234 Mt yr⁻¹. To synthesize the observed patterns of morphological evolution from the inner estuary to the outer subaqueous delta, it can be inferred that most portion of the subaqueous delta has most likely experienced accretion-erosion conversion. The mouth bar area showed the lowest sensitivity to fluvial sediment decline among portions of the delta due to its intrinsic characteristics as a sediment accumulating site. With a likely further decrease in SD and new land reclamation projects planned within the mouth bar

area, delta erosion is likely to continue in the future. Adaptive strategies to counter these threats to estuarine ecosystems and engineering facilities are thus urgently needed for delta sustainability.

Declaration of competing interest

The authors declare that they have no known competing financial interests or personal relationships that could have appeared to influence the work reported in this paper.

Acknowledgments

This paper is a product of the project “Coping with deltas in transition” within the Programme of Strategic Scientific Alliances between China and The Netherlands (PSA), financed by the Chinese Ministry of Science and Technology (MOST), Project no. 2016YFE0133700 and Royal Netherlands Academy of Arts and Sciences (KNAW), Project no. PSA-SA-E-02. This study was also financed by the Ministry of Science and Technology of China (2016YFA0600903), the Open Research Fund of State Key Laboratory of Estuarine and Coastal Research (SKLEC-PGKF201905), the National Natural Science Foundation of China (42006156, 52009008), the Fundamental Research Funds for Central Public Welfare Research Institutes (CKSF2019167/HL), the Key Project of the Shanghai Science & Technology Committee (17DJ14003) and the Natural Science Foundation of China-Shandong Joint Fund for Marine Science Research Centers (U1606401). The bathymetry data used in this study are gratefully provided by Navigation Guarantee Department of the Chinese Navy Headquarters, Shanghai Waterway Bureau of Ministry of Transport and Yangtze Estuary Waterway Administration Bureau of Ministry of Transport. The authors are grateful to the editor and four anonymous reviewers for their thoughtful and constructive comments and suggestions.

Appendix A. Supplementary data

Supplementary data to this article can be found online at <https://doi.org/10.1016/j.geomorph.2021.107680>.

References

- Anthony, E.J., Brunier, G., Besset, M., Goichot, M., Dussouillez, P., Nguyen, V.L., 2015. Linking rapid erosion of the Mekong River delta to human activities. *Sci. Rep.* 5, 14745.
- Bittencourt, A.C.D.S., Dominguez, J.M.L., Fontes, L.C.S., Sousa, D.L., Silva, I.R., Da Silva, F.R., 2007. Wave refraction, river damming, and episodes of severe shoreline erosion: the São Francisco River Mouth, Northeastern Brazil. *J. Coast. Res.* 23 (4), 930–938.
- Blott, S.J., Pye, K., van der Wal, D., Neal, A., 2006. Long-term morphological change and its causes in the Mersey Estuary, NW England. *Geomorphology* 81, 185–206.
- Blum, M.D., Roberts, H.H., 2012. The Mississippi delta region: past, present, and future. *Annu. Rev. Earth Planet. Sci.* 40, 655–683.
- Canestrelli, A., Fagherazzi, S., Defina, A., Lanzoni, S., 2010. Tidal hydrodynamics and erosional power in the Fly River delta, Papua New Guinea. *J. Geophys. Res. Earth Surf.* 115, F4033.
- Chen, J., Zhu, H., Dong, Y., Sun, J., 1985. Development of the Changjiang estuary and its submerged delta. *Cont. Shelf Res.* 4, 47–56.
- Chen, J., Li, D., Chen, B., Hu, F., Zhu, H., Liu, C., 1999. The processes of dynamic sedimentation in the Changjiang Estuary. *J. Sea Res.* 41, 129–140.
- Chen, Z.Y., Xu, K., Watanabe, M., 2007. Dynamic hydrology and geomorphology of the Yangtze River. In: Gupta, A. (Ed.), *Large Rivers: Geomorphology and Management*. Wiley, England, pp. 457–469.
- Chu, Z.X., Sun, X.G., Zhai, S.K., Xu, K.H., 2006. Changing pattern of accretion/erosion of the modern Yellow River (Huanghe) subaerial delta, China: based on remote sensing images. *Mar. Geol.* 227, 13–30.
- Dai, Z., Liu, J.T., Fu, G., Xie, H., 2013. A thirteen-year record of bathymetric changes in the North Passage, Changjiang (Yangtze) estuary. *Geomorphology* 187, 101–107.
- Dai, Z., Liu, J.T., Wei, W., Chen, J., 2014. Detection of the Three Gorges Dam influence on the Changjiang (Yangtze River) submerged delta. *Sci. Rep.* 4, 6600.
- Dai, Z., Fagherazzi, S., Mei, X., Chen, J., Meng, Y., 2016. Linking the infilling of the North Branch in the Changjiang (Yangtze) estuary to anthropogenic activities from 1958 to 2013. *Mar. Geol.* 379, 1–12.
- Day, J.W., Agboola, J., Chen, Z.D., Elia, C., Forbes, D.L., Giosan, L., Kemp, P., Kuenzer, C., Lane, R.R., Ramachandran, R., Syvitski, J., Yañez-Arancibia, A., 2016. Approaches to defining deltaic sustainability in the 21st century. *Estuar. Coast. Shelf Sci.* 183 (Part B), 275–291.
- De Vriend, H., Wang, Z., Ysebaert, T., Herman, P.J., Ding, P., 2011. Eco-morphological problems in the Yangtze Estuary and the Western Scheldt. *Wetlands* 31, 1033–1042.
- Deng, B., Wu, H., Yang, S., Zhang, J., 2017. Longshore suspended sediment transport and its implications for submarine erosion off the Yangtze River Estuary. *Estuar. Coast. Shelf Sci.* 190, 1–10.
- Du, J., Yang, S., Feng, H., 2016. Recent human impacts on the morphological evolution of the Yangtze River delta foreland: a review and new perspectives. *Estuar. Coast. Shelf Sci.* 181, 160–169.
- Duan, G.L., 2012. *Study on the Different Computation Patterns on Riverbed Erosion and Deposition Amount*. Wuhan University, Wuhan.
- Edmonds, D.A., Slingerland, R.L., 2007. Mechanics of river mouth bar formation: implications for the morphodynamics of delta distributary networks. *J. Geophys. Res.* 112 (F2).
- Giosan, L., Syvitski, J., Constantinescu, S., Day, J., 2014. Climate change: protect the world's deltas. *Nature* 516, 31–33.
- Guo, L.C., 2014. *Modeling Estuarine Morphodynamics under Combined River and Tidal Forcing*. UNESCO-IHE, Delft.
- Hori, K., Saito, Y., Zhao, Q., Cheng, X., Wang, P., Sato, Y., Li, C., 2001. Sedimentary facies and Holocene progradation rates of the Changjiang (Yangtze) delta, China. *Geomorphology* 41, 233–248.
- Jaffe, B.E., Smith, R.E., Foxgrover, A.C., 2007. Anthropogenic influence on sedimentation and intertidal mudflat change in San Pablo Bay, California: 1856–1983. *Estuar. Coast. Shelf Sci.* 73, 175–187.
- Jay, D.A., Musiak, J.D., 1994. Particle trapping in estuarine tidal flows. *J. Geophys. Res. Oceans* 99 (C10), 20445–20461.
- Jia, J., Gao, J., Cai, T., Li, Y., Yang, Y., Wang, Y.P., Xia, X., Li, J., Wang, A., Gao, S., 2018. Sediment accumulation and retention of the Changjiang (Yangtze River) subaqueous delta and its distal muds over the last century. *Mar. Geol.* 401, 2–16.
- Jiang, C., Pan, S., Chen, S., 2017. Recent morphological changes of the Yellow River (Huanghe) submerged delta: causes and environmental implications. *Geomorphology* 293, 93–107.
- Li, X., Liu, J.P., Tian, B., 2016. Evolution of the Jiuduansha wetland and the impact of navigation works in the Yangtze Estuary, China. *Geomorphology* 253, 328–339.
- Liu, X., Cui, D., 2019. Study on deposition characteristics of promoting silting project in the Yangtze Estuary. *J. Sediment. Res.* 44 (1), 24–30 (in Chinese).
- Liu, J.P., Xu, K.H., Li, A.C., Milliman, J.D., Velozzi, D.M., Xiao, S.B., Yang, Z.S., 2007. Flux and fate of Yangtze River sediment delivered to the East China Sea. *Geomorphology* 85, 208–224.
- Liu, H., He, Q., Wang, Z., Weltje, G.J., Zhang, J., 2010. Dynamics and spatial variability of near-bottom sediment exchange in the Yangtze Estuary, China. *Estuar. Coast. Shelf Sci.* 86, 322–330.
- Luan, H.L., Ding, P.X., Wang, Z.B., Ge, J.Z., Yang, S.L., 2016. Decadal morphological evolution of the Yangtze Estuary in response to river input changes and estuarine engineering projects. *Geomorphology* 265, 12–23.
- Luan, H.L., Ding, P.X., Wang, Z.B., Ge, J.Z., 2017. Process-based morphodynamic modeling of the Yangtze Estuary at a decadal timescale: controls on estuarine evolution and future trends. *Geomorphology* 290, 347–364.
- Luan, H.L., Ding, P.X., Wang, Z.B., Yang, S.L., Lu, J.Y., 2018. Morphodynamic impacts of large-scale engineering projects in the Yangtze River delta. *Coast. Eng.* 141, 1–11.
- Luo, X.X., Yang, S.L., Zhang, J., 2012. The impact of the Three Gorges Dam on the downstream distribution and texture of sediments along the middle and lower Yangtze River (Changjiang) and its estuary, and subsequent sediment dispersal in the East China Sea. *Geomorphology* 179, 126–140.
- Luo, X.X., Yang, S.L., Wang, R.S., Zhang, C.Y., Li, P., 2017. New evidence of Yangtze delta recession after closing of the Three Gorges Dam. *Sci. Rep.* 7, 41735.
- Maloney, J.M., Bentley, S.J., Xu, K., Obelcz, J., Georgiou, I.Y., Miner, M.D., 2018. Mississippi River subaqueous delta is entering a stage of retrogradation. *Mar. Geol.* 400, 12–23.
- Milliman, J.D., Farnsworth, K.L., 2011. *River Discharge to the Coastal Ocean: A Global Synthesis*. Cambridge University Press, Cambridge.
- Morton, R.A., Bernier, J.C., Barras, J.A., Ferina, N.F., 2005. Rapid Subsidence and Historical Wetland Loss in the Mississippi Delta Plain: Likely Causes and Future Implications. *US Geol. Surv.*, Washington, DC.
- Preoteasa, L., Vespremeanu-Stroe, A., Tăuți, F., Zăinescu, F., Alida, T., Cîrdan, I., 2016. The evolution of an asymmetric deltaic lobe (Sf. Gheorghe, Danube) in association with cyclic development of the river-mouth bar: long-term pattern and present adaptations to human-induced sediment depletion. *Geomorphology* 253, 59–73.
- Renaud, F.G., Syvitski, J.P., Sebesvari, Z., Werners, S.E., Kremer, H., Kuenzer, C., Ramesh, R., Jeuken, A., Friedrich, J., 2013. Tipping point from the Holocene to the Anthropocene: how threatened are major world deltas? *Curr. Opin. Environ. Sustain.* 5, 644–654.
- Stanley, D.J., Chen, Z., 1993. Yangtze delta, eastern China: 1. Geometry and subsidence of Holocene deposcenter. *Mar. Geol.* 112, 1–11.
- Syvitski, J.P.M., Saito, Y., 2007. Morphodynamics of deltas under the influence of humans. *Glob. Planet. Chang.* 57, 261–282.
- Syvitski, J.P.M., Kettner, A.J., Overeem, I., Hutton, E.W.H., Hannon, M.T., Brakenridge, G.R., Day, J., Vorosmarty, C., Saito, Y., Giosan, L., Nicholls, R.J., 2009. Sinking deltas due to human activities. *Nat. Geosci.* 2, 681–686.
- Tessler, Z.D., Vorosmarty, C.J., Grossberg, M., Gladkova, I., Aizenman, H., Syvitski, J.P.M., Foufoula-Georgiou, E., 2015. Profiling risk and sustainability in coastal deltas of the world. *Science* 349, 638–643.
- Van der Wal, D., Pye, K., Neal, A., 2002. Long-term morphological change in the Ribble Estuary, northwest England. *Mar. Geol.* 189, 249–266.
- Wang, J., Gao, W., Xu, S., et al., 2012. Evaluation of the combined risk of sea level rise, land subsidence, and storm surges on the coastal areas of Shanghai, China. *Clim. Chang.* 115 (3–4), 537–558.

- Wang, Z.B., Van Maren, D.S., Ding, P.X., Yang, S.L., Van Prooijen, B.C., De Vet, P.L.M., Winterwerp, J.C., De Vriend, H.J., Stive, M.J.F., He, Q., 2015. Human impacts on morphodynamic thresholds in estuarine systems. *Cont. Shelf Res.* R3681.
- Wei, W., Mei, X., Dai, Z., Tang, Z., 2016. Recent morphodynamic evolution of the largest uninhibited island in the Yangtze (Changjiang) estuary during 1998–2014: influence of the anthropogenic interference. *Cont. Shelf Res.* 124, 83–94.
- Wei, W., Dai, Z., Mei, X., Liu, J.P., Gao, S., Li, S., 2017. Shoal morphodynamics of the Changjiang (Yangtze) estuary: influences from river damming, estuarine hydraulic engineering and reclamation projects. *Mar. Geol.* 386, 32–43.
- Wei, W., Dai, Z., Mei, X., Gao, S., Liu, J.P., 2019. Multi-decadal morpho-sedimentary dynamics of the largest Changjiang estuarine marginal shoal: causes and implications. *Land Degrad. Dev.* 30, 2048–2063.
- White, K., El Asmar, H.M., 1999. Monitoring changing position of coastlines using Thematic Mapper imagery, an example from the Nile Delta. *Geomorphology* 29, 93–105.
- Wright, L.D., 1977. Sediment transport and deposition at river mouths: a synthesis. *Geol. Soc. Am. Bull.* 88, 857–868.
- Wright, L.D., Coleman, J.M., 1974. Mississippi river mouth processes: effluent dynamics and morphologic Development. *J. Geol.* 82 (6), 751–778.
- Wu, Z., Li, Z., Zhao, M., 2003. The process and prediction of sea level change of China offshore waters in 50 years. *Hydrographic surveying and charting.* 23 (2), 17–19 (in Chinese).
- Wu, Z., Milliman, J.D., Zhao, D., et al., 2018. Geomorphologic changes in the lower Pearl River Delta, 1850–2015, largely due to human activity. *Geomorphology* 314, 42–54.
- Xie, D., Pan, C., Wu, X., et al., 2017. Local human activities overwhelm decreased sediment supply from the Changjiang River: continued rapid accumulation in the Hangzhou Bay-Qiantang Estuary system. *Mar. Geol.* 392, 66–77.
- Yang, S.L., Belkin, I.M., Belkina, A.I., Zhao, Q.Y., Zhu, J., Ding, P.X., 2003. Delta response to decline in sediment supply from the Yangtze River: evidence of the recent four decades and expectations for the next half-century. *Estuar. Coast. Shelf Sci.* 57, 689–699.
- Yang, S.L., Zhang, J., Zhu, J., Smith, J.P., Dai, S.B., Gao, A., Li, P., 2005. Impact of dams on Yangtze River sediment supply to the sea and delta intertidal wetland response. *J. Geophys. Res. Earth Surf.* 110, F3006.
- Yang, S.L., Milliman, J.D., Li, P., Xu, K., 2011. 50,000 dams later: erosion of the Yangtze River and its delta. *Glob. Planet. Chang.* 75, 14–20.
- Yang, S.L., Milliman, J.D., Xu, K.H., Deng, B., Zhang, X.Y., Luo, X.X., 2014. Downstream sedimentary and geomorphic impacts of the Three Gorges Dam on the Yangtze River. *Earth-Sci. Rev.* 138, 469–486.
- Yang, S.L., Xu, K.H., Milliman, J.D., Yang, H.F., Wu, C.S., 2015. Decline of Yangtze River water and sediment discharge: impact from natural and anthropogenic changes. *Sci. Rep.* 5, 12581.
- Yang, H.F., Yang, S.L., Xu, K.H., Wu, H., Shi, B.W., 2017. Erosion potential of the Yangtze Delta under sediment starvation and climate change. *Sci. Rep.* 7, 10535.
- Yang, H.F., Yang, S.L., Xu, K.H., Milliman, J.D., Wang, H., Yang, Z., Chen, Z., Zhang, C.Y., 2018. Human impacts on sediment in the Yangtze River: a review and new perspectives. *Glob. Planet. Chang.* 162, 8–17.
- Yang, H.F., Yang, S.L., Meng, Y., Xu, K.H., Luo, X.X., Wu, C.S., Shi, B.W., 2018b. Recent coarsening of sediments on the southern Yangtze subaqueous delta front: a response to river damming. *Cont. Shelf Res.* 155, 45–51.
- Yang, S.L., Luo, X., Temmerman, S., Kirwan, M., Bouma, T., Xu, K., Zhang, S., Fan, J., Shi, B., Yang, H., Wang, Y.P., Shi, X., Gao, S., 2020. Role of delta-front erosion in sustaining salt marshes under sea-level rise and fluvial sediment decline. *Limnol. Oceanogr.* 9999, 1–20.
- Yun, C., 2004. *Recent Evolution of Yangtze Estuary and Its Mechanisms.* China Ocean Press, Beijing, China (in Chinese).
- Zhang, M., Townend, I., Cai, H., He, J., Mei, X., 2018. The influence of seasonal climate on the morphology of the mouth-bar in the Yangtze Estuary, China. *Cont. Shelf Res.* 153, 30–49.
- Zhu, L., He, Q., Shen, J., Wang, Y., 2016. The influence of human activities on morphodynamics and alteration of sediment source and sink in the Changjiang Estuary. *Geomorphology* 273, 52–62.
- Zhu, C., Guo, L., Maren, D.S., Tian, B., Wang, X., He, Q., Wang, Z.B., 2019. Decadal morphological evolution of the mouth zone of the Yangtze Estuary in response to human interventions. *Earth Surf. Proc. Land* 44, 2319–2332.